

# Infrared fixed point of QCD, critical flavor number and triality automorphism of octonions

Sadataka Furui

*School of Science and Engineering, Teikyo University.*

*1-1 Toyosatodai, Utsunomiya, 320-8551 Japan*

## Abstract

We show that the discrepancy on the critical flavor number of fermions  $N_f^c$  for the appearance of the infrared fixed point based on the t'Hooft anomaly matching condition and derived from the Schrödinger functional method ( $N_f^c \sim 9$ ) and the experimental analysis of the JLab group using Bjorken sum rule and GDH sum rule, and our lattice simulation ( $N_f^c \sim 3$ ) could be resolved by assuming the topological structure of the infrared fixed point is not that of  $U(1)^3$  but that of  $G_2$  with triality automorphism of octonions which appear in the product of quaternions.

The relation between the infrared fixed point of the running coupling measured in lattice simulations and the prediction of the BLM renormalization theory, the role of fermions in the Kugo-Ojima color confinement, and the quaternion real condition are also discussed.

PACS numbers: 12.38.Gc, 12.38.Aw, 11.10.Gh, 11.15.Ha, 11.15.Tk, 11.30.Rd

## I. INTRODUCTION

Infrared QCD is characterized by spontaneous chiral symmetry breaking. The quark field of QCD at low energy is expressed as[1]

$$\psi = \frac{1}{2}(1 + \gamma_5)\psi_L + \frac{1}{2}(1 - \gamma_5)\psi_R \quad (1)$$

where  $\psi_L$  transforms as  $SU(3)$  color under  $G_c$ ,  $SU(N)_L$  flavor under  $G_F$  and  $SL(2, c)$  Lorentz spinor and  $\psi_R$  transforms as  $SU(3)$  color,  $SU(2)_R$  flavor and  $SL(2, c)$  Lorentz spinor.

Color gauge fields bind these quarks into baryons which must be color singlets. In the model that gauge group  $G_c$  coupled to chiral fermions, the representation of the group must be such that the anomaly is cancelled. In the space of symmetry  $G_c \times G_F$ , t'Hooft considered

$$G_F = SU(n_1)_L \otimes SU(n_2)_R \otimes SU(n_3)_L \otimes SU(n_4)_R \otimes U(1)^3 \quad (2)$$

where  $n_{1,2}$  refer to the triplets and  $n_{3,4}$  to sextets.

t'Hooft proposed anomaly matching relation in which the symmetric anomaly coefficient  $d^{abc}$  contributed from the massless quarks should be equal to the coefficient  $D^{abc}$  contributed from the massless color singlet composite fermions [1].

The approach up to fermionic degrees of freedom  $N_f = 5$  was not successful, but an algebraic research was extensively done in [2], and it is shown that the matching of  $SU(N_f)_L^2 \times U(1)_B$  and  $SU(N_f)_R^2 \times U(1)_B$  anomalies, where  $U_B(1)$  is the vector-like Baryon number, and matching of  $SU(N_f)_L^3$  and  $SU(N_f)_R^3$  anomalies can be done in  $N_f \pm 6$  dimensional representation [3]. The condition on  $SU(N_f)_L^3$  and  $SU(N_f)_R^3$  anomalies is

$$3 = -(N_f \pm 6) + \frac{1}{2}(N_f \pm 3)(N_f \pm 6) + \frac{1}{2}N_f(N_f \pm 1) - N_f(N_f \pm 4) \quad (3)$$

and that for  $SU(N_f)_L^2 U_B(1)$  and  $SU(N_f)_R^2 U_B(1)$  anomalies is

$$1 = -(N_f \pm 6) \frac{N_f \pm 2}{N_f \pm 6} + \frac{1}{2}(N_f \pm 2)(N_f \pm 3) + \frac{1}{2}N_f(N_f \pm 1) - N_f(N_f \pm 2). \quad (4)$$

where  $U_B(1)$  is the baryon number charge. It means that QCD with 3 flavor and 3 color system cannot satisfy the matching condition.

Sannino [4] found another solution that satisfies the anomaly matching condition in  $2N_f \pm 15$  dimensional system, which requires  $N_f > 8$ . He found the condition for a  $SU(N_f)_L^3$  anomalies as

$$3 = -(2N_f \pm 15) + \frac{1}{2}(N_f \pm 3)(N_f \pm 6) + \frac{1}{2}N_f(N_f \pm 1) - N_f(N_f \pm 4) \quad (5)$$

and that for  $SU(N_f)_L^2 U_V(1)$  anomalies as

$$1 = -(2N_f \pm 15) \frac{2N_f \pm 5}{2N_f \pm 15} + \frac{1}{2}(N_f \pm 2)(N_f \pm 3) + \frac{1}{2}N_f(N_f \pm 1) - N_f(N_f \pm 2) \quad (6)$$

where  $U_V(1)$  is the vector charge.

The critical number of flavors for opening the conformal window and the critical number of flavors for presence of infrared fixed point is expected to be close to each other. A study of infrared fixed point was done on the lattice by measuring the momentum dependence of the QCD running coupling.

In the perturbative  $\beta$  function and DSE approach, infrared fixed point  $\alpha_{IR}$  is a decreasing function of number of flavors  $N_f$ . When  $\alpha_{IR}$  decreases below the minimal value of  $\alpha_{cr}$  for which the fermion acquires a mass, the  $N_f$  is called  $N_f^c$ [8, 10]. Near this  $N_f$ , the effective coupling varies slowly as the momentum changes. Lattice simulation of  $N_c = 3$ [5] suggests  $N_f^c \sim 7$ , while more recent lattice simulation [6, 7] and DSE[8] suggest that  $8 < N_f^c \leq 12$ .

Recently Appelquist[6, 7] claimed by performing lattice simulation of running coupling in the Schrödinger functional method [9] that there is a critical number of flavors  $N_f^c$  below which both chiral symmetry breaking and confinement set in. He assigned  $8 \leq N_f^c \leq 12$  and in the case of  $N_f = 8$  the running coupling monotonically increase as  $\beta$  decreases and in the case of  $16^4$  lattice and  $\beta \sim 4.65$ ,  $g^2(L)/4\pi \sim 20/4\pi \sim 1.7$ , and that there is no sign of infrared fixed point. However, the Schrödinger functional method  $\alpha_s(q)$  is parametrized as  $\frac{c}{\log q/\Lambda} + \dots$  and its applicability in the region of  $q$  below and around  $\Lambda \sim 213 \pm 40\text{MeV}$  is not clear. Brodsky et al, [10, 11] argue that in the DSE  $q < \Lambda$  or  $r > 1\text{fm}$ , and in ADS/QCD  $\zeta = \sqrt{\mathbf{b}_\perp x(1-x)} > \lambda_{max} \sim 1\text{fm}$ , confinement is essential and the quark-gluon should not be treated as free.

On the lattice, the QCD running coupling was also measured by using the propagators of gluon, ghost and quarks. In Landau gauge and in Coulomb gauge, we measured  $\alpha_s(q)$  via ghost-gluon coupling[12, 13] and via quark-gluon coupling [14]. In the case of ghost-gluon coupling, we calculated the product of the ghost propagator and the gluon propagator and observed infrared suppression due to suppression of the ghost propagator. The ghost propagator in the Landau gauge has color antisymmetric part whose expectation value is 0 but its norm becomes comparable to that of color diagonal part in the infrared [15]. This kind of problem is absent in the Coulomb gauge. The lattice data calculated by using the gauge configuration of MILC[16] and RBC/UKQCD[17] suggest an infrared fixed point of

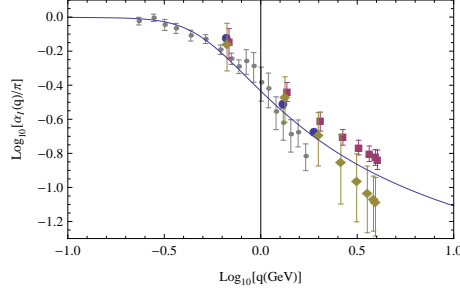


FIG. 1: The running coupling of the domain wall fermion. Coulomb gauge gluon-ghost coupling of  $m_u = 0.01/a$ (square),  $0.02/a$ (diamond), and quark-gluon coupling of  $m_u = 0.01/a$ (large disks). Small disks are the  $\alpha_{s,g1}$  derived from the spin structure function of the JLab group[19]and the solid curve is their fit.

$\alpha_s(0) \simeq 3$  in the case of Coulomb gauge domain wall fermion of  $16^3 \times 32 \times 16$  [14].

Experimentally the JLab group [18, 19] showed that the data of spin structure function of a proton and a neutron and the Bjorken sum rule [20] and the Drell-Hearn-Gerasimov sum rule[21, 22]. and the formula of Brodsky-Lepage-Mackenzie(BLM) scheme[23, 24] strongly suggests a presence of infrared fixed point of  $\alpha_s(0) = \pi$  and the effective coupling has walking like behavior near infrared. In the BLM scheme, observables A and B are related in terms of the effective charge as

$$\alpha_A(Q_A) = \alpha_B(Q_B) \left( 1 + r_{A/B} \frac{\alpha_B}{\pi} + \dots \right) \quad (7)$$

and the coefficient  $r_{A/B}$  is so chosen that the result does not depend on the number of flavors  $N_f$ .

We show in Fig. 1 the lattice simulation of the domain wall fermion and the JLab results.

In our lattice simulation of  $N_f = 2+1$ ,  $\alpha_s(q) \sim 1.7$  at  $q \sim 0.6\text{GeV}$  and the deviation of the running coupling from 2-loop perturbative calculation is significant below  $q \sim 3\text{GeV}$  due to  $A^2$  condensates [25, 26]. I think the non-perturbative effect is significant in the infrared and the Schrödinger functional method do not disprove the infrared fixed point at  $N_f = 2 + 1$ . In [10, 11], the origin of appearance of the infrared fixed point is attributed to the acquiring of mass of the gluon and decoupling of the gluon polarization effects.

The organization of the paper is as follows. In sect.2, the octonion and anomaly matching condition are explained. We explain our method of gauge fixing of the gluon and domain wall fermion system in sect.3. The form factor of the proton calculated by this gauge fixing

is presented in sect.4.

We discuss whether our finding of infrared fixed point in  $N_f = 2 + 1$  lattice simulation is incompatible with the estimates of Schrödinger functional method and give conclusions in sect.5.

## II. OCTONION AND ANOMALY MATCHING CONDITION

In the vector like theory that  $SU(N_f)_L^2 \times U(1)_V$  and  $SU(N_f)_R^2 \times U(1)_V$  anomalies and  $SU(N_f)_L^3$  and  $SU(N_f)_R^3$  anomalies can be matched in  $2N_f \pm 5N_c$  dimensional representation[4]. The model of [4] may be regarded as magnetic dual of the gauge theory. The factor 5 in this QCD dual may be related to the  $1/N_c$  corrections to the one body matrix elements in the Skyrme model[27] which was necessary to reproduce magnetic transition of a nucleon to  $\Delta$ . These condition  $N_f - 6 = 3$  and  $2N_f - 15 = 3$  are both satisfied by  $N_f = 9$ , but the standard model of QCD predicts  $N_f = 3$ .

The quadratic form of quaternion is expressed by octonion, and the automorphism in the space of octonion is  $G_2$  group which is exceptional Lie group with 14 dimensional representation. In  $G_2$ , there is a specific automorphism, which is called triality. In the following subsection, we study the structure of the  $G_2$  group.

### A. Representation theory of $G_2$ group

In this subsection, we study the quaternion and the representation theory of  $G_2$ [28].

A quaternion  $q \in \mathbf{H}$  can be defined by using the basis  $\{1, \mathbf{i}, \mathbf{j}, \mathbf{k}\} = \{I, i\sigma_1, i\sigma_2, i\sigma_3\}$  as  $q = wI + ix\sigma_1 + iy\sigma_2 + iz\sigma_3$ , where  $\sigma_i$  are Pauli matrices and  $I = 1^2$  is the unit matrix. As a complex number is expressed by a product of real numbers

$$(x_1, y_1)(x_2, y_2) = (x_1x_2 - y_1y_2, x_1y_2 + y_1x_2)$$

a quaternion is expressed by a product of complex numbers

$$(z_1, w_1)(z_2, w_2) = (z_1z_2 - w_1\bar{w}_2, z_1w_2 + w_1\bar{z}_2)$$

The quaternion  $\mathbf{H}$  and a new imaginary unit  $\mathbf{l}$  that anti-commute with  $\mathbf{i}, \mathbf{j}, \mathbf{k}$  compose an octonion  $\mathbf{O} = \mathbf{H} + \mathbf{lH}$ . It is spanned by

$$\{1, \mathbf{i}, \mathbf{j}, \mathbf{k}, \mathbf{l}, \mathbf{il}, \mathbf{jl}, \mathbf{kl}\} = \{1, \mathbf{e}_1, \mathbf{e}_2, \mathbf{e}_3, \mathbf{e}_4, \mathbf{e}_5, \mathbf{e}_6, \mathbf{e}_7\}$$

with bases of Clifford algebra  $\mathbf{O} = \mathbf{R} + \mathbf{R}^7$ .

An octonion is expressed as a product of quaternions

$$(p_1, q_1) \circ (p_2, q_2) = (p_1 p_2 - \bar{q}_2 q_1, q_2 p_1 + q_1 \bar{p}_2) \quad (8)$$

The algebra  $\mathbf{O}$  is associated with an involution[29]

$$g \rightarrow \check{g} = \begin{pmatrix} 1 & 0 \\ 0 & -{}^7 1 \end{pmatrix} g \begin{pmatrix} 1 & 0 \\ 0 & -{}^7 1 \end{pmatrix} \quad (9)$$

where  ${}^7 1$  is the 7 dimensional diagonal matrix. In the subspace  $\mathbf{R}^7$ , automorphisms of  $SO(7)$  are of the form  $U \rightarrow SUS^{-1}$  where  $S \in SO(7)$ . Automorphism of  $\mathbf{Spin}(7)$  are of the form  $u \rightarrow sus^{-1}$ .

In the space  $\mathbf{R}^8$ , automorphism of  $Spin(8)$  is expressed as injection

$$\mathbf{R}^8 \rightarrow {}^2\mathbf{R}(8) : a \begin{pmatrix} v(a) & 0 \\ 0 & {}^t v(a) \end{pmatrix} \quad (10)$$

whose image is defined as  $\mathbf{Y}$ . For an element  $y \in \mathbf{Y}$  and the unit element  $g \in \mathbf{O}$ , involution  $\check{g}$  of  $g$  is defined as

$$\check{g} y \mathbf{e} = \overline{\check{g} y \mathbf{e}}. \quad (11)$$

where  $\overline{y \mathbf{e}}$  is the complex conjugation of  $y \mathbf{e}$ . When the element  $g$  satisfies  $g \mathbf{e} = \mathbf{e}$  and  $\check{g}$  also satisfies  $\check{g} \mathbf{e} = \mathbf{e}$ ,  $\check{g}$  is called the companion element of  $g$ .

In the case of  $SO(8)$ , with  $g_0$  and the companion of  $g_1$ , an element of  $Spin(8)$  is  $\begin{pmatrix} g_0 & 0 \\ 0 & \check{g}_1 \end{pmatrix}$  and by the definition of  $g_2$  of

$$g_0 y \check{g}_1^{-1} \mathbf{e} = \check{g}_2 y \mathbf{e} \quad (12)$$

for all  $y \in \mathbf{Y}$ , one can construct a triple  $(g_0, g_1, g_2)$ .

The triality automorphism is

$$\theta : Spin(8) \rightarrow Spin(8); \begin{pmatrix} g_0 & 0 \\ 0 & \check{g}_1 \end{pmatrix} \rightarrow \begin{pmatrix} g_1 & 0 \\ 0 & \check{g}_2 \end{pmatrix} \quad (13)$$

Triality transformation rotates 24 dimensional bases defined by Cartan[30].

$$\{\xi_0, \xi_1, \xi_2, \xi_3, \xi_4\}, \quad \{\xi_{12}, \xi_{31}, \xi_{23}, \xi_{14}, \xi_{24}, \xi_{34}\}, \quad \{\xi_{123}, \xi_{124}, \xi_{314}, \xi_{234}, \xi_{1234}\}$$

$$\{x^1, x^2, x^3, x^4\}, \quad \{x^{1'}, x^{2'}, x^{3'}, x^{4'}\}$$

The trilinear form in these bases is

$$\begin{aligned} \mathcal{F} &= \phi^T C X \psi = x^1(\xi_{12}\xi_{314} - \xi_{31}\xi_{124} - \xi_{14}\xi_{123} + \xi_{1234}\xi_1) \\ &+ x^2(\xi_{23}\xi_{124} - \xi_{12}\xi_{234} - \xi_{24}\xi_{123} + \xi_{1234}\xi_2) \\ &+ x^3(\xi_{31}\xi_{234} - \xi_{23}\xi_{314} - \xi_{34}\xi_{123} + \xi_{1234}\xi_3) \\ &+ x^4(-\xi_{14}\xi_{234} - \xi_{24}\xi_{314} - \xi_{34}\xi_{124} + \xi_{1234}\xi_4) \\ &+ x^{1'}(-\xi_0\xi_{234} + \xi_{23}\xi_4 - \xi_{24}\xi_3 + \xi_{34}\xi_2) \\ &+ x^{2'}(-\xi_0\xi_{314} + \xi_{31}\xi_4 - \xi_{34}\xi_1 + \xi_{14}\xi_3) \\ &+ x^{3'}(-\xi_0\xi_{124} + \xi_{12}\xi_4 - \xi_{14}\xi_2 + \xi_{24}\xi_1) \\ &+ x^{4'}(\xi_0\xi_{123} - \xi_{23}\xi_1 - \xi_{31}\xi_2 - \xi_{12}\xi_3) \end{aligned} \quad (14)$$

There are three semi-spinors which have quadratic form which is invariant with respect to the group of rotation

$${}^t\phi C \phi = \xi_0\xi_{1234} - \xi_{23}\xi_{14} - \xi_{31}\xi_{24} - \xi_{12}\xi_{34} \quad (15)$$

$${}^t\psi C \psi = \xi_1\xi_{234} - \xi_2\xi_{134} - \xi_3\xi_{124} - \xi_4\xi_{123} \quad (16)$$

and the vector

$$F = x^1x^{1'} + x^2x^{2'} + x^3x^{3'} + x^4x^{4'} \quad (17)$$

The triality transformation that makes  $g\mathbf{e} = \mathbf{e}$  for  $\mathbf{e} = x^1, x^2, x^3$  and  $x^{1'}, x^{2'}, x^{3'}$  is defined as  $G_{23}$ ,  $g\mathbf{e} = \mathbf{e}$  for  $\mathbf{e} = \xi_1, \xi_2, \xi_3$  and  $\xi_{124}, \xi_{314}, \xi_{234}$  is defined as  $G_{12}$ ,  $g\mathbf{e} = \mathbf{e}$  for  $\mathbf{e} = \xi_{12}, \xi_{31}, \xi_{23}$  and  $\xi_{14}, \xi_{24}, \xi_{34}$  is defined as  $G_{13}$ . In addition to  $G_{23}, G_{12}$  and  $G_{13}$ , there are automorphism  $G_{12}G_{13} = G_{132}$  and  $G_{13}G_{12} = G_{123}$ .

When one defines for each  $i = 0, 1, 2$

$$H_i = \{(g_0, g_1, g_2) \in Spin(8) : g_i\mathbf{e} = \mathbf{e}\},$$

the triality transformation is expressed as  $\theta(H_0) = H_1, \theta(H_1) = H_2$  and  $\theta(H_2) = H_0$ , and  $G_2 = H_1 \cap H_2 = H_2 \cap H_0 = H_0 \cap H_1$ [29].

In the space of octonions, we choose  $\xi_1$  as an element orthogonal to 1, and  $\xi_2$  as an element orthogonal to 1 and  $\xi_1$ , and  $\xi_4$  as an element orthogonal to 1,  $\xi_1, \xi_2$  and  $\xi_1\xi_2$ . For orthogonal elements  $\xi_1, \xi_2, \xi_4$  chosen as  $\xi_k$ , there is an automorphism  $\xi_1 \rightarrow \xi_{14}, \xi_2 \rightarrow \xi_{24}, \xi_4 \rightarrow \xi_0$ . The

choice of  $\xi_{14}$  is a choice of a point on a unit sphere in the 7 dimensional space,  $\xi_{24}$  is a choice of a point on a unit sphere in the 6 dimensional space, and  $\xi_0$  is a choice in the space orthogonal to  $1, \xi_{14}, \xi_{24}, \xi_{14}\xi_{24}$  i.e. in the 4 dimensional space. These form 6, 5 and 3 dimensional manifolds. The exceptional Lie group representation  $G_2$  is the automorphism in this 14 dimensional manifold.

We assign  $SU(3)$  fundamental color representation of quarks on the 3 dimensional manifolds and that of the color representation of diquarks on the 6 dimensional manifolds and 4 dimensional spinors and 1 dimensional space between spins on the domain walls to the 5 dimensional manifold. The triality transformation mixes the 3 and 6 dimensional spaces.

Irreducible representations of  $g_2$  algebra with highest weight  $a\omega_1 + b\omega_2$  is written as  $\Gamma_{a,b}$ , and we study the standard representation  $V = \Gamma_{1,0}$ .

## B. Anomaly matching condition

A problem is whether the anomaly matching of the color triplet and color sextet sectors in a baryon can be explicitly realized. The fundamental representation of the  $g_2$  algebra has 14 vectors

$$g_2 = \{H_1, H_2, X_1, Y_1, X_2, Y_2, X_3, Y_3, X_4, Y_4, X_5, Y_5, X_6, Y_6\}$$

One can define a subgroup

$$g_0 = \{H_5, H_2, X_5, Y_5, X_2, Y_2, X_6, Y_6\},$$

where  $H_5 = H_1 + H_2$ , which is isomorphic to  $sl_3(C)$ [28].

The rest of the Lie algebra consists of

$$W = \{X_4, Y_1, Y_3\} \quad \text{and} \quad W^* = \{Y_4, X_1, X_3\}$$

When a representation has the highest weight  $\omega_1 = 2\alpha_1 + \alpha_2$  it is seven dimensional, we call it  $V$ . The wedge product  $\wedge^2 V$  is

$$\wedge^2 V \simeq \Gamma_{0,1} + V$$

and  $\wedge^3 V$  is

$$\wedge^3 V \simeq \Gamma_{2,0} + V + \mathbf{C}$$

where  $\mathbf{C}$  is the trivial representation.



The action of  $g_2$  on the standard representation preserves a skew-symmetric trilinear form  $\omega$  on  $V$ , which consists of

$$\omega = w_3 \wedge u \wedge v_3 + v_4 \wedge u \wedge w_4 + w_1 \wedge u \wedge v_1 + 2v_1 \wedge v_3 \wedge w_4 + 2w_1 \wedge w_3 \wedge v_4 \quad (18)$$

where with use of root vectors  $Y_1$  and  $Y_2$ ,  $v_3 = Y_1(v_4)$ ,  $v_1 = -Y_2(v_3)$ ,  $u = Y_1(v_1)$ ,  $w_1 = Y_1(u)/2$ ,  $w_3 = Y_2(w_1)$  and  $w_4 = -Y_1(w_3)$ . It means that the five-dimensional space  $\omega$  is stable in  $\wedge^3 V$ , and that the anomaly matching relation of the massless fermion state and the bound state of three massless fermion which is given by  $\wedge^3 V$  can be considered in the same five dimensional space.

$su(3)$  is a subalgebra of  $sl_3(C)$ , but it is real representation. The quaternion real condition imposed on the quark propagator has the effect of constraining  $sl_3(C)$  to its real representation  $su(3)$ . Anomaly matching relation on the massless fermion and the bound state of three massless fermions with flavor  $N_f = 3$  and color  $N_c = 3$  could be interpreted as the  $N_f = 9$  without triality, since the same 5 dimensional space appears 3 times through triality transformation. The topology around the infrared fixed point would be more complicated than the  $U(1)^3$ .

### III. GAUGE FIXING OF THE DOMAIN WALL FERMION

We first perform gauge fixing in Landau gauge using the overrelaxation method and then fix to the Coulomb gauge without touching the  $A_4$  component[32]. We then measure the quark propagator and fix the gauge in the space of the 5th dimension between the domain walls.

In the analysis of instantons in quaternion bases, Corrigan and Goddard [31] defined the transition function  $g(\omega, \pi)$  where  $\omega$  and  $\pi$  are complex two-spinors which satisfy

$$g(\lambda\omega, \lambda\pi) = g(\omega, \pi), \quad \det g = 1.$$

@When  $\omega = x\pi$  where  $x = x^0 - i\mathbf{x} \cdot \boldsymbol{\sigma}$ ,  $g(\omega, \pi)$  is a quaternion can be expressed as

$$g(x\pi, \pi) = h(x, \zeta)k(x, \zeta)^{-1}$$

where  $\zeta = \frac{\pi_1}{\pi_2}$ ,  $h(x, \zeta)$  is regular in  $|\zeta| > 1 - \epsilon$  and  $k(x, \zeta)$  is regular in  $|\zeta| < 1 + \epsilon$ .

In [31], the Ansatz

$$\begin{aligned} g_0 &= \begin{pmatrix} e^{-\nu} & 0 \\ 0 & e^{\nu} \end{pmatrix} \begin{pmatrix} \zeta^1 & \rho \\ 0 & \zeta^{-1} \end{pmatrix} \begin{pmatrix} e^{\mu} & 0 \\ 0 & e^{-\mu} \end{pmatrix} \\ &= \begin{pmatrix} e^{\gamma} \zeta^1 & f(\gamma, \zeta) \\ 0 & e^{-\gamma} \zeta^{-1} \end{pmatrix} \end{aligned} \quad (19)$$

was proposed as the transformation matrix. In our 5-dimensional domain wall fermion case,  $\gamma = \mu - \nu$  and  $\mu, \nu$  contain the phase in the 5th direction  $i\eta$ .

$$2\mu = i\omega_2/\pi_2 - i\eta = (x_1 + ix_2)\zeta + ix_0 - x_3 - i\eta \quad (20)$$

$$2\nu = i\omega_1/\pi_1 + i\eta = (x_1 - ix_2)\zeta + ix_0 + x_3 + i\eta \quad (21)$$

The quaternion reality condition of the transformation matrix  $g(\gamma, \zeta)$  gives

$$\begin{pmatrix} a_{L_s-1} & b_{L_s-1} \\ c_{L_s-1} & d_{L_s-1} \end{pmatrix} \begin{pmatrix} \zeta^1 e^{\gamma} & f \\ 0 & \zeta^{-1} e^{-\gamma} \end{pmatrix} = \begin{pmatrix} \zeta^1 e^{-\gamma} & \bar{f} \\ 0 & \zeta^{-1} e^{\gamma} \end{pmatrix} \begin{pmatrix} a_0 & b_0 \\ c_0 & d_0 \end{pmatrix} \quad (22)$$

where  $\bar{f} = \overline{f(\bar{\gamma}, -\frac{1}{\bar{\zeta}})}$ .

The function  $f$  and  $\bar{f}$  taken in [31] is

$$f = \frac{d_0 e^{\gamma} - \frac{1}{a_{L_s-1}} e^{-\gamma}}{\psi}, \quad \bar{f} = \frac{\frac{1}{d_{L_s-1}} e^{\gamma} - a_0 e^{-\gamma}}{\psi}.$$

In general  $c_0$  and  $c_{L_s-1}$  are polynomials of  $\zeta$ , and they satisfy  $c_{L_s-1} \zeta^1 = c_0 \zeta^{-1}$ . We define

$$\psi = \hat{c}_{-1} \zeta^{-1} + \hat{c}_1 \zeta^1 + \delta$$

where  $\hat{c}_{-1} = c_{L_s-1}$  and  $\hat{c}_1 = c_0$  and  $\delta$  is a constant, which is defined later.

With the Ansatz  $\psi = c_0 \zeta^{-1} + c_{L_s-1} \zeta^1 + \delta$ , we find  $\zeta^1 = \sqrt{\frac{c_0}{c_{L_s-1}}}$  and the  $e^{\gamma}$  and the  $\delta$  are calculated from the simultaneous equation (III):

$$\begin{cases} a_{L_s-1} f + b_{L_s-1} \zeta^{-1} e^{-\gamma} = b_0 \zeta^{-1} e^{-\gamma} + d_0 \bar{f} \\ c_{L_s-1} f + d_{L_s-1} \zeta^{-1} e^{-\gamma} = d_0 \zeta^{-1} e^{\gamma}. \end{cases}$$

The equation has two sets of solutions which can be obtained numerically.

We assign  $\begin{pmatrix} a_0 & b_0 \\ c_0 & d_0 \end{pmatrix}_{L/R}$  and  $\begin{pmatrix} a_{L_s-1} & b_{L_s-1} \\ c_{L_s-1} & d_{L_s-1} \end{pmatrix}_{L/R}$  from the color diagonal components of the lattice data.

From the numerical practice, we observe that the deviation  $\Delta L/R$  becomes small when the  $|\delta|$  is large, i.e. when  $\psi \sim \delta \sim \frac{1}{f}$  is large. It means that  $e^{2\gamma} \sim \frac{d_{L_s-1}}{d_0}$  is a good approximation in the case of small deviation, and we select the gauge such that the corresponding  $|\delta|$  is large.

#### IV. FORM FACTOR OF THE PROTON

With the prescription on the gauge of fermions on the domain walls, we calculate the baryon charge form factor of a proton using the SU(6) spin-flavor wave function. The nucleon three point function is

$$\begin{aligned} & \langle G^{NV_\mu N}(t_2, t_1; \mathbf{p} + \frac{\mathbf{q}}{2}, \mathbf{p} - \frac{\mathbf{q}}{2}; \Gamma) \rangle \\ &= \sum_{\mathbf{x}} e^{-i(\mathbf{p} + \frac{\mathbf{q}}{2}) \cdot \mathbf{x}_2} e^{i(\mathbf{p} - \frac{\mathbf{q}}{2}) \cdot \mathbf{x}_1} \times \Gamma^{\beta\alpha} \langle \Omega | T[\chi^\alpha(\mathbf{x}_2, t_2) V_\mu(\mathbf{0}, 0) \bar{\chi}^\beta(\mathbf{x}_1, -t_1)] | \Omega \rangle \end{aligned}$$

where

$$\chi(x) = \epsilon^{abc} [u^{Ta}(x) C \gamma_5 d^b(x)] u^c(x)$$

In these expressions  $abc$  specify colors,  $\alpha$  and  $\beta$  specify spin dependent  $A$  term or spin independent  $B$  term of each three quark propagators.

In the limit of  $t_1 \rightarrow -\infty, t_2 \rightarrow +\infty$ , the fourier transform reduces to the vertex sandwiched by the propagators.

The nucleon two-point function is

$$\langle G^{NN}(t_2, t_1, \mathbf{p}; \Gamma) \rangle = \sum_{\mathbf{x}} e^{-i\mathbf{p} \cdot \mathbf{x}_2} e^{i\mathbf{p} \cdot \mathbf{x}_1} \Gamma^{\beta\alpha} \langle \Omega | T \chi^\alpha(\mathbf{x}_2, t_2) \bar{\chi}^\beta(\mathbf{x}_1, t_1) | \Omega \rangle.$$

We take the limit of  $t_1 \rightarrow -\infty, t_2 \rightarrow +\infty$ , here also. We define the S-matrix as

$$S(a, h_a, a, h'_a | p) = S^A(a, h_a, a, h'_a | p) + S^B(a, h_a, a, h'_a | p), \quad (23)$$

where

$$\begin{aligned} S^A(a, h_a, a, h'_a | p) &= \frac{-i\mathcal{A}p}{\mathcal{A}p^2 + \mathcal{M}\mathcal{B}} \Big|_{h_a, h'_a} \\ S^B(a, h_a, a, h'_a | p) &= \frac{\mathcal{B}}{\mathcal{A}p^2 + \mathcal{M}\mathcal{B}} \Big|_{h_a, h'_a} \end{aligned}$$

In the coupling of  $V_\mu$  to  $(u^a(x) C \gamma_5 d^b(x)) u^c(x)$  and  $(u^{a'}(x) C \gamma_5 d^{b'}(x)) u^{c'}(x)$ , we evaluate the real part of

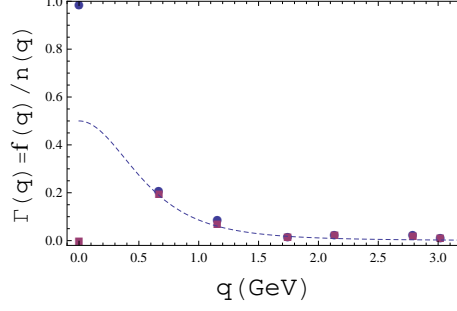


FIG. 2: The form factor of a proton using the DWF  $m_u = 0.01/a$  gauge fixed such that the fermion on the left wall and the right wall are correlated by self-dual gauge field, and the dipole fit with  $M^2 = 0.71\text{GeV}^2$ . At zero momentum left-handed(LH) fermion dominates the form factor, and at finite momentum, LH and RH contribute almost equally.

1.  $S^\alpha(c, h_c, c, h'_c|p)u^c_{h'_c}(p)V_\mu u^c_{h^*_c}(p) \times \gamma_5 S^\beta(c, h^*_c, c, h|p)^\dagger \gamma_5$
2.  $S^\alpha(a, h_a, a, h'_a|p)u^a_{h'_a}(p)V_\mu u^a_{h^*_a}(p) \times \gamma_5 S^\beta(a, h^*_a, a, h_a|p)^\dagger \gamma_5$
3.  $S^\alpha(b, -h_b, b, -h'_b|-p)^\dagger u^b_{h'_b}(-p)V_\mu u^b_{h^*_b}(-p) \times \gamma_5 S^\beta(b, -h^*_b, b, -h_b|-p)\gamma_5$

We used the fact that the helicity of  $C\gamma_5 d(x)$  becomes negative of the original.

The expectation values of the charge form factor  $G_{c+}^{NVN}$  is

$$\Gamma(q) = \frac{1}{2} \left[ \frac{G_{c+}^{NVN}(p, q)}{G_{c+}^{NN}(p, q)} + \frac{G_{c-}^{NVN}(p, q)}{G_{c-}^{NN}(p, q)} + \frac{G_{a+}^{NVN}(p, q)}{G_{a+}^{NN}(p, q)} + \frac{G_{a-}^{NVN}(p, q)}{G_{a-}^{NN}(p, q)} + \frac{G_{b-}^{NVN}(p, q)}{G_{b-}^{NN}(p, q)} + \frac{G_{b+}^{NVN}(p, q)}{G_{b+}^{NN}(p, q)} \right]$$

At zero momentum the left-handed quark contribution dominates when the gauge fixing parity on the domain wall fermion is applied. When the gauge fixing parity is not applied, the left-handed quark and the right handed quark give almost the same contribution.

We show in Fig. 2, the form factor of the proton of the domain wall fermion of  $16^3 \times 32 \times 16$  lattice of  $ud$ - quark mass  $0.01/a$  (148 samples). The momentum  $\mathbf{q}$  is chosen to be  $(q_1, q_2, q_3, q_4) = (0, 0, 0, 0), (1, 0, 0, 0), (1, 1, 1, 0), (4, 0, 0, 0), (2, 2, 2, 0), (3, 3, 3, 0), (4, 4, 4, 0)$ .

The dotted line is the dipole fit with  $\lambda = 0.71\text{GeV}$ . Since the contribution of left handed and right-handed are almost the same for  $q \neq 0$  the fitted line is normalized to be 0.5 at  $q = 0$ .

## V. DISCUSSION AND CONCLUSION

We showed that the discrepancy on the critical flavor number of fermions  $N_f^c$  for the appearance of the infrared fixed point derived from the Schrödinger functional method and the Bjorken sum rule and GDH sum rule and our lattice simulation could be resolved by assuming the topological structure of the infrared fixed point is not that of  $U(1)^3$  but that of  $G_2$  with triality automorphism.

The Lie algebra  $g_2$  has the 8 dimensional subspace  $g_0$  which is isomorphic to  $sl_3(C)$  and the 3 dimensional subspace  $W$  and  $W^*$ .  $sl_3(C)$  is not isomorphic to  $su(3)$ , but by imposing quaternion real condition, the subspace isomorphic to  $su(3)$  would be selected.

The lattice simulation of QCD running coupling from quark-gluon coupling in Coulomb gauge suggests infrared fixed point of  $\alpha_s(0) \sim \pi$  which is predicted in BLM renormalization scheme. The strong interaction sum rules obtained in the infinite momentum frame with holographic variable  $z$  in addition to the 3+1 dimensional space time is 5 dimensional and similar to ours.

In Landau gauge the running coupling from ghost-gluon coupling near infrared is ambiguous due to fluctuation of the ghost propagator. Gribov[46] discussed the role of anomalous current in which fermionic zero modes contribute to stabilize IR fluctuation of the gauge field

$$j_\kappa^e = -\frac{\epsilon^2}{32\pi^3} \int \frac{d\Omega}{(\epsilon z)^2} d^{abc} F_{\kappa\nu}^a(x) A_\nu^b(x, z) \quad (24)$$

where  $d^{abc}$  is the color SU(3) structure factor and  $F_{\kappa\nu}^a$  is the tensor constructed by the fermionic zero modes.

Effects of instanton on  $\mathbf{S}^3 \times \mathbf{R}$  topology in Coulomb gauge was studied in the quaternion bases[47]. We observed that the self-dual gauge field (instanton) plays important roles in the stability of the infrared QCD. In lattice simulations without gauge fixing[41], the  $\|Q\| = 1$  instanton was not detected, but it is due to the difficulty of detecting a topological feature which appears in the infinite volume and does not contradict with our findings.

Using the domain wall fermion in quaternion bases, and taking into account that the quadratic term of quaternion makes an octonion, we remarked that there are 3,6 and 5 dimensional stable manifolds and the exceptional Lie algebra  $g_2$  is the automorphism in this space. The  $g_2$  has triality automorphism and the topology of the infrared fixed point is not trivial. We extended [39] and [40] to larger number of gauge configurations, and calculated

the form factor of the proton choosing a specific gauge that the fermion on the left domain wall and the right domain wall are correlated by the instanton-like self-dual gauge fields.

Recently, the Kugo-Ojima color confinement attracted renewed interest by a conjecture of possible BRST (Becchi-Rouet-Stora-Tyutin) symmetry breaking in the infrared [36–38]. These authors pay attention to the restriction of the gauge configuration to the fundamental modular region defined by Zwanziger to solve the Gribov problem[42, 43]. The Kugo-Ojima confinement parameter  $u(0)$  becomes -1, and the Gribov-Zwanziger horizon function  $h(0)$  becomes 0, are equivalent. There is an argument that the free boundary condition which is defined as  $Q_0(t) = \sum_{\mathbf{x}} A_0(t, \mathbf{x}) = 0$  on the boundary, guarantees the horizon function becomes 0[44]. The free boundary condition is derived from the Landau gauge condition and transversality condition, but it is not guaranteed that one can gauge transform all configurations to satisfy the free boundary condition.

Kondo[37] parametrized the horizon function

$$\langle (gf^{abc} A_\mu^b c^c)(gf^{def} A_\nu^e \bar{c}^f) \rangle_k = -\delta^{ad} \left( \delta_{\mu\nu}^T u(q^2) + F(q^2) \frac{q_\mu q_\nu}{q^2} (u(q^2) + w(q^2)) \right) \quad (25)$$

and assuming  $w(0) = 0$ , obtained  $u(0) = -2/3$ .

We find that in the quenched lattice simulation, Kugo-Ojima confinement criterion is not satisfied, and that the solution  $u(0) = -2/3, w(0) = 0$  obtained in the DSE [37] which suggests BRST violation[36] in the quenched calculations are possible in contrast to [45]. By including dynamical fermions, however, we found that  $u(0)$  is consistent with -1, which implies importance of fermions in the confinement. Our lattice simulation does not guarantee that the gauge configurations have reached the fundamental modular region, but we checked in quenched relatively small lattice that the results of lattice Landau gauge Kugo-Ojima parameter does not drastically change by Parallel Tempering gauge fixing[32]. In view of complex topology near the infrared fixed point, one could ask whether one should seek gauge uniqueness in the quenched infrared QCD simulation.

We measured the form factor in Coulomb gauge with an assumption of correlation between domain wall fermions by a quaternion real gauge field with a reduction  $U(3) \rightarrow SU(3) \otimes U_B(1)$ . Incorporation of symmetry breaking of  $U_V(1)$ , i.e.  $Q_u = 2/3, Q_d = Q_s = -1/3$  is under investigation.

## Acknowledgments

I would like to thank Dr. Francesco Sannino for valuable information on the anomaly matching, Professor Stan Brodsky for attracting attention to the ref. [10] and helpful discussion, and Dr. Alex Deur for sending me the experimental data. The numerical simulation was performed on Hitachi-SR11000 at High Energy Accelerator Research Organization(KEK) under a support of its Large Scale Simulation Program (No.07-04 and No.08-01), and on NEC-SX8 at Yukawa institute of theoretical physics of Kyoto University.

## VI. APPENDIX: $\gamma$ MATRICES AND TRIALITY

I use the  $\gamma$  matrices, as follows:

$$\gamma_k = \begin{pmatrix} 0 & i\sigma_k \\ -i\sigma_k & 0 \end{pmatrix}, \quad \gamma_5 = \begin{pmatrix} 1 & 0 & 0 & 0 \\ 0 & 1 & 0 & 0 \\ 0 & 0 & -1 & 0 \\ 0 & 0 & 0 & -1 \end{pmatrix}, \quad \gamma_4 = \begin{pmatrix} 0 & 0 & 1 & 0 \\ 0 & 0 & 0 & 1 \\ 1 & 0 & 0 & 0 \\ 0 & 1 & 0 & 0 \end{pmatrix}$$

$$\gamma_1 = \begin{pmatrix} 0 & 0 & 0 & i \\ 0 & 0 & i & 0 \\ 0 & -i & 0 & 0 \\ -i & 0 & 0 & 0 \end{pmatrix}, \quad \gamma_2 = \begin{pmatrix} 0 & 0 & 0 & -1 \\ 0 & 0 & 1 & 0 \\ 0 & 1 & 0 & 0 \\ -1 & 0 & 0 & 0 \end{pmatrix}, \quad \gamma_3 = \begin{pmatrix} 0 & 0 & i & 0 \\ 0 & 0 & 0 & -i \\ -i & 0 & 0 & 0 \\ 0 & i & 0 & 0 \end{pmatrix},$$

$$\gamma_4\gamma_2\gamma_5 = \begin{pmatrix} 0 & 1 & 0 & 0 \\ -1 & 0 & 0 & 0 \\ 0 & 0 & 0 & 1 \\ 0 & 0 & -1 & 0 \end{pmatrix}, \quad \gamma_4\gamma_2 = \begin{pmatrix} 0 & 1 & 0 & 0 \\ -1 & 0 & 0 & 0 \\ 0 & 0 & 0 & -1 \\ 0 & 0 & 1 & 0 \end{pmatrix},$$

$$\gamma_4\gamma_1\gamma_5 = \begin{pmatrix} 0 & -i & 0 & 0 \\ -i & 0 & 0 & 0 \\ 0 & 0 & 0 & -i \\ 0 & 0 & -i & 0 \end{pmatrix}, \quad \gamma_4\gamma_3\gamma_5 = \begin{pmatrix} -i & 0 & 0 & 0 \\ 0 & i & 0 & 0 \\ 0 & 0 & -i & 0 \\ 0 & 0 & 0 & i \end{pmatrix}$$



The matrix elements of the triality transformation of the  $g_2$  algebra.  $G_{23}, G_{12}, G_{13}$  are copied from Cartan's book.  $\bar{1}$  indicates -1. In  $G_{23}$ , I replaced  $\xi_3 \rightarrow \xi_{34}$  written in [30] (probably a typo) to  $\xi_3 \rightarrow -\xi_{34}$ .  $G_{132} = G_{13}G_{12}$  and  $G_{123} = G_{12}G_{13}$  are also added.

$G_{23}$

	$\xi_0$	$\xi_1$	$\xi_2$	$\xi_3$	$\xi_4$	$\xi_{12}$	$\xi_{31}$	$\xi_{23}$	$\xi_{14}$	$\xi_{24}$	$\xi_{34}$	$\xi_{123}$	$\xi_{124}$	$\xi_{314}$	$\xi_{234}$	$\xi_{1234}$	$x^1$	$x^2$	$x^3$	$x^4$	$x^{1'}$	$x^{2'}$	$x^{3'}$	$x^{4'}$
$\xi_0$	0	0	0	0	1	0	0	0	0	0	0	0	0	0	0	0	0	0	0	0	0	0	0	0
$\xi_1$	0	0	0	0	0	0	0	0	$\bar{1}$	0	0	0	0	0	0	0	0	0	0	0	0	0	0	0
$\xi_2$	0	0	0	0	0	0	0	0	0	$\bar{1}$	0	0	0	0	0	0	0	0	0	0	0	0	0	0
$\xi_3$	0	0	0	0	0	0	0	0	0	0	$\bar{1}$	0	0	0	0	0	0	0	0	0	0	0	0	0
$\xi_4$	$\bar{1}$	0	0	0	0	0	0	0	0	0	0	0	0	0	0	0	0	0	0	0	0	0	0	0
$\xi_{12}$	0	0	0	0	0	0	0	0	0	0	0	0	1	0	0	0	0	0	0	0	0	0	0	0
$\xi_{31}$	0	0	0	0	0	0	0	0	0	0	0	0	0	1	0	0	0	0	0	0	0	0	0	0
$\xi_{23}$	0	0	0	0	0	0	0	0	0	0	0	0	0	0	1	0	0	0	0	0	0	0	0	0
$\xi_{14}$	0	1	0	0	0	0	0	0	0	0	0	0	0	0	0	0	0	0	0	0	0	0	0	0
$\xi_{24}$	0	0	1	0	0	0	0	0	0	0	0	0	0	0	0	0	0	0	0	0	0	0	0	0
$\xi_{34}$	0	0	0	1	0	0	0	0	0	0	0	0	0	0	0	0	0	0	0	0	0	0	0	0
$\xi_{123}$	0	0	0	0	0	0	0	0	0	0	0	0	0	0	0	$\bar{1}$	0	0	0	0	0	0	0	0
$\xi_{124}$	0	0	0	0	0	$\bar{1}$	0	0	0	0	0	0	0	0	0	0	0	0	0	0	0	0	0	0
$\xi_{314}$	0	0	0	0	0	0	$\bar{1}$	0	0	0	0	0	0	0	0	0	0	0	0	0	0	0	0	0
$\xi_{234}$	0	0	0	0	0	0	0	$\bar{1}$	0	0	0	0	0	0	0	0	0	0	0	0	0	0	0	0
$\xi_{1234}$	0	0	0	0	0	0	0	0	0	0	0	1	0	0	0	0	0	0	0	0	0	0	0	0
$x^1$	0	0	0	0	0	0	0	0	0	0	0	0	0	0	0	0	1	0	0	0	0	0	0	0
$x^2$	0	0	0	0	0	0	0	0	0	0	0	0	0	0	0	0	0	1	0	0	0	0	0	0
$x^3$	0	0	0	0	0	0	0	0	0	0	0	0	0	0	0	0	0	0	1	0	0	0	0	0
$x^4$	0	0	0	0	0	0	0	0	0	0	0	0	0	0	0	0	0	0	0	0	0	0	0	$\bar{1}$
$x^{1'}$	0	0	0	0	0	0	0	0	0	0	0	0	0	0	0	0	0	0	0	0	1	0	0	0
$x^{2'}$	0	0	0	0	0	0	0	0	0	0	0	0	0	0	0	0	0	0	0	0	0	1	0	0
$x^{3'}$	0	0	0	0	0	0	0	0	0	0	0	0	0	0	0	0	0	0	0	0	0	0	1	0
$x^{4'}$	0	0	0	0	0	0	0	0	0	0	0	0	0	0	0	0	0	0	0	$\bar{1}$	0	0	0	0

$G_{12}$ 

	$\xi_0$	$\xi_1$	$\xi_2$	$\xi_3$	$\xi_4$	$\xi_{12}$	$\xi_{31}$	$\xi_{23}$	$\xi_{14}$	$\xi_{24}$	$\xi_{34}$	$\xi_{123}$	$\xi_{124}$	$\xi_{314}$	$\xi_{234}$	$\xi_{1234}$	$x^1$	$x^2$	$x^3$	$x^4$	$x^{1'}$	$x^{2'}$	$x^{3'}$	$x^{4'}$	
$\xi_0$	0	0	0	0	0	0	0	0	0	0	0	0	0	0	0	0	0	0	0	1	0	0	0	0	
$\xi_1$	0	1	0	0	0	0	0	0	0	0	0	0	0	0	0	0	0	0	0	0	0	0	0	0	0
$\xi_2$	0	0	1	0	0	0	0	0	0	0	0	0	0	0	0	0	0	0	0	0	0	0	0	0	0
$\xi_3$	0	0	0	1	0	0	0	0	0	0	0	0	0	0	0	0	0	0	0	0	0	0	0	0	0
$\xi_4$	0	0	0	0	0	0	0	0	0	0	0	0	0	0	0	$\bar{1}$	0	0	0	0	0	0	0	0	0
$\xi_{12}$	0	0	0	0	0	0	0	0	0	0	0	0	0	0	0	0	0	0	1	0	0	0	0	0	0
$\xi_{31}$	0	0	0	0	0	0	0	0	0	0	0	0	0	0	0	0	0	1	0	0	0	0	0	0	0
$\xi_{23}$	0	0	0	0	0	0	0	0	0	0	0	0	0	0	0	0	1	0	0	0	0	0	0	0	0
$\xi_{14}$	0	0	0	0	0	0	0	0	0	0	0	0	0	0	0	0	0	0	0	0	$\bar{1}$	0	0	0	0
$\xi_{24}$	0	0	0	0	0	0	0	0	0	0	0	0	0	0	0	0	0	0	0	0	0	$\bar{1}$	0	0	0
$\xi_{34}$	0	0	0	0	0	0	0	0	0	0	0	0	0	0	0	0	0	0	0	0	0	0	$\bar{1}$	0	0
$\xi_{123}$	0	0	0	0	$\bar{1}$	0	0	0	0	0	0	0	0	0	0	0	0	0	0	0	0	0	0	0	0
$\xi_{124}$	0	0	0	0	0	0	0	0	0	0	0	0	1	0	0	0	0	0	0	0	0	0	0	0	0
$\xi_{314}$	0	0	0	0	0	0	0	0	0	0	0	0	0	1	0	0	0	0	0	0	0	0	0	0	0
$\xi_{234}$	0	0	0	0	0	0	0	0	0	0	0	0	0	0	1	0	0	0	0	0	0	0	0	0	0
$\xi_{1234}$	0	0	0	0	0	0	0	0	0	0	0	0	0	0	0	0	0	0	0	0	0	0	0	0	1
$x^1$	0	0	0	0	0	0	0	$\bar{1}$	0	0	0	0	0	0	0	0	0	0	0	0	0	0	0	0	0
$x^2$	0	0	0	0	0	0	$\bar{1}$	0	0	0	0	0	0	0	0	0	0	0	0	0	0	0	0	0	0
$x^3$	0	0	0	0	0	$\bar{1}$	0	0	0	0	0	0	0	0	0	0	0	0	0	0	0	0	0	0	0
$x^4$	$\bar{1}$	0	0	0	0	0	0	0	0	0	0	0	0	0	0	0	0	0	0	0	0	0	0	0	0
$x^{1'}$	0	0	0	0	0	0	0	0	$\bar{1}$	0	0	0	0	0	0	0	0	0	0	0	0	0	0	0	0
$x^{2'}$	0	0	0	0	0	0	0	0	0	$\bar{1}$	0	0	0	0	0	0	0	0	0	0	0	0	0	0	0
$x^{3'}$	0	0	0	0	0	0	0	0	0	0	$\bar{1}$	0	0	0	0	0	0	0	0	0	0	0	0	0	0
$x^{4'}$	0	0	0	0	0	0	0	0	0	0	0	0	0	0	0	$\bar{1}$	0	0	0	0	0	0	0	0	0

$G_{13}$ 

	$\xi_0$	$\xi_1$	$\xi_2$	$\xi_3$	$\xi_4$	$\xi_{12}$	$\xi_{31}$	$\xi_{23}$	$\xi_{14}$	$\xi_{24}$	$\xi_{34}$	$\xi_{123}$	$\xi_{124}$	$\xi_{314}$	$\xi_{234}$	$\xi_{1234}$	$x^1$	$x^2$	$x^3$	$x^4$	$x^{1'}$	$x^{2'}$	$x^{3'}$	$x^{4'}$	
$\xi_0$	0	0	0	0	0	0	0	0	0	0	0	0	0	0	0	$\bar{1}$	0	0	0	0	0	0	0	0	
$\xi_1$	0	0	0	0	0	0	0	0	0	0	0	0	0	0	0	0	0	0	0	0	0	1	0	0	0
$\xi_2$	0	0	0	0	0	0	0	0	0	0	0	0	0	0	0	0	0	0	0	0	0	0	1	0	0
$\xi_3$	0	0	0	0	0	0	0	0	0	0	0	0	0	0	0	0	0	0	0	0	0	0	0	1	0
$\xi_4$	0	0	0	0	0	0	0	0	0	0	0	0	0	0	0	0	0	0	0	0	0	0	0	0	1
$\xi_{12}$	0	0	0	0	0	1	0	0	0	0	0	0	0	0	0	0	0	0	0	0	0	0	0	0	0
$\xi_{31}$	0	0	0	0	0	0	1	0	0	0	0	0	0	0	0	0	0	0	0	0	0	0	0	0	0
$\xi_{23}$	0	0	0	0	0	0	0	1	0	0	0	0	0	0	0	0	0	0	0	0	0	0	0	0	0
$\xi_{14}$	0	0	0	0	0	0	0	0	1	0	0	0	0	0	0	0	0	0	0	0	0	0	0	0	0
$\xi_{24}$	0	0	0	0	0	0	0	0	0	1	0	0	0	0	0	0	0	0	0	0	0	0	0	0	0
$\xi_{34}$	0	0	0	0	0	0	0	0	0	0	1	0	0	0	0	0	0	0	0	0	0	0	0	0	0
$\xi_{123}$	0	0	0	0	0	0	0	0	0	0	0	0	0	0	0	0	0	0	0	0	1	0	0	0	0
$\xi_{124}$	0	0	0	0	0	0	0	0	0	0	0	0	0	0	0	0	0	0	0	$\bar{1}$	0	0	0	0	0
$\xi_{314}$	0	0	0	0	0	0	0	0	0	0	0	0	0	0	0	0	0	0	$\bar{1}$	0	0	0	0	0	0
$\xi_{234}$	0	0	0	0	0	0	0	0	0	0	0	0	0	0	0	0	$\bar{1}$	0	0	0	0	0	0	0	0
$\xi_{1234}$	$\bar{1}$	0	0	0	0	0	0	0	0	0	0	0	0	0	0	0	0	0	0	0	0	0	0	0	0
$x^1$	0	0	0	0	0	0	0	0	0	0	0	0	0	0	1	0	0	0	0	0	0	0	0	0	0
$x^2$	0	0	0	0	0	0	0	0	0	0	0	0	0	1	0	0	0	0	0	0	0	0	0	0	0
$x^3$	0	0	0	0	0	0	0	0	0	0	0	0	1	0	0	0	0	0	0	0	0	0	0	0	0
$x^4$	0	0	0	0	0	0	0	0	0	0	0	$\bar{1}$	0	0	0	0	0	0	0	0	0	0	0	0	0
$x^{1'}$	0	$\bar{1}$	0	0	0	0	0	0	0	0	0	0	0	0	0	0	0	0	0	0	0	0	0	0	0
$x^{2'}$	0	0	$\bar{1}$	0	0	0	0	0	0	0	0	0	0	0	0	0	0	0	0	0	0	0	0	0	0
$x^{3'}$	0	0	0	$\bar{1}$	0	0	0	0	0	0	0	0	0	0	0	0	0	0	0	0	0	0	0	0	0
$x^{4'}$	0	0	0	0	$\bar{1}$	0	0	0	0	0	0	0	0	0	0	0	0	0	0	0	0	0	0	0	0

$G_{132}$ 

	$\xi_0$	$\xi_1$	$\xi_2$	$\xi_3$	$\xi_4$	$\xi_{12}$	$\xi_{31}$	$\xi_{23}$	$\xi_{14}$	$\xi_{24}$	$\xi_{34}$	$\xi_{123}$	$\xi_{124}$	$\xi_{314}$	$\xi_{234}$	$\xi_{1234}$	$x^1$	$x^2$	$x^3$	$x^4$	$x^{1'}$	$x^{2'}$	$x^{3'}$	$x^{4'}$
$\xi_0$	0	0	0	0	0	0	0	0	0	0	0	$\bar{1}$	0	0	0	0	0	0	0	0	0	0	0	0
$\xi_1$	0	0	0	0	0	0	0	0	0	0	0	0	0	0	0	0	0	0	0	0	1	0	0	0
$\xi_2$	0	0	0	0	0	0	0	0	0	0	0	0	0	0	0	0	0	0	0	0	0	1	0	0
$\xi_3$	0	0	0	0	0	0	0	0	0	0	0	0	0	0	0	0	0	0	0	0	0	0	1	0
$\xi_4$	1	0	0	0	0	0	0	0	0	0	0	0	0	0	0	0	0	0	0	0	0	0	0	0
$\xi_{12}$	0	0	0	0	0	0	0	0	0	0	0	0	1	0	0	0	0	0	0	0	0	0	0	0
$\xi_{31}$	0	0	0	0	0	0	0	0	0	0	0	0	0	1	0	0	0	0	0	0	0	0	0	0
$\xi_{23}$	0	0	0	0	0	0	0	0	0	0	0	0	0	0	1	0	0	0	0	0	0	0	0	0
$\xi_{14}$	0	1	0	0	0	0	0	0	0	0	0	0	0	0	0	0	0	0	0	0	0	0	0	0
$\xi_{24}$	0	0	1	0	0	0	0	0	0	0	0	0	0	0	0	0	0	0	0	0	0	0	0	0
$\xi_{34}$	0	0	0	1	0	0	0	0	0	0	0	0	0	0	0	0	0	0	0	0	0	0	0	0
$\xi_{123}$	0	0	0	0	0	0	0	0	0	0	0	0	0	0	0	0	0	0	0	0	0	0	0	$\bar{1}$
$\xi_{124}$	0	0	0	0	0	0	0	0	0	0	0	0	0	0	0	0	0	0	$\bar{1}$	0	0	0	0	0
$\xi_{314}$	0	0	0	0	0	0	0	0	0	0	0	0	0	0	0	0	0	$\bar{1}$	0	0	0	0	0	0
$\xi_{234}$	0	0	0	0	0	0	0	0	0	0	0	0	0	0	0	0	$\bar{1}$	0	0	0	0	0	0	0
$\xi_{1234}$	0	0	0	0	$\bar{1}$	0	0	0	0	0	0	0	0	0	0	0	0	0	0	0	0	0	0	0
$x^1$	0	0	0	0	0	0	0	$\bar{1}$	0	0	0	0	0	0	0	0	0	0	0	0	0	0	0	0
$x^2$	0	0	0	0	0	0	$\bar{1}$	0	0	0	0	0	0	0	0	0	0	0	0	0	0	0	0	0
$x^3$	0	0	0	0	0	$\bar{1}$	0	0	0	0	0	0	0	0	0	0	0	0	0	0	0	0	0	0
$x^4$	0	0	0	0	0	0	0	0	0	0	0	0	0	0	0	1	0	0	0	0	0	0	0	0
$x^{1'}$	0	0	0	0	0	0	0	0	$\bar{1}$	0	0	0	0	0	0	0	0	0	0	0	0	0	0	0
$x^{2'}$	0	0	0	0	0	0	0	0	0	$\bar{1}$	0	0	0	0	0	0	0	0	0	0	0	0	0	0
$x^{3'}$	0	0	0	0	0	0	0	0	0	0	$\bar{1}$	0	0	0	0	0	0	0	0	0	0	0	0	0
$x^{4'}$	1	0	0	0	0	0	0	0	0	0	0	0	0	0	0	0	0	0	0	0	0	0	0	0

$G_{123}$

	$\xi_0$	$\xi_1$	$\xi_2$	$\xi_3$	$\xi_4$	$\xi_{12}$	$\xi_{31}$	$\xi_{23}$	$\xi_{14}$	$\xi_{24}$	$\xi_{34}$	$\xi_{123}$	$\xi_{124}$	$\xi_{314}$	$\xi_{234}$	$\xi_{1234}$	$x^1$	$x^2$	$x^3$	$x^4$	$x^{1'}$	$x^{2'}$	$x^{3'}$	$x^{4'}$	
$\xi_0$	0	0	0	0	0	0	0	0	0	0	0	0	0	0	0	0	0	0	0	0	0	0	0	0	$\bar{1}$
$\xi_1$	0	0	0	0	0	0	0	0	$\bar{1}$	0	0	0	0	0	0	0	0	0	0	0	0	0	0	0	0
$\xi_2$	0	0	0	0	0	0	0	0	0	$\bar{1}$	0	0	0	0	0	0	0	0	0	0	0	0	0	0	0
$\xi_3$	0	0	0	0	0	0	0	0	0	0	$\bar{1}$	0	0	0	0	0	0	0	0	0	0	0	0	0	0
$\xi_4$	0	0	0	0	0	0	0	0	0	0	0	0	0	0	0	$\bar{1}$	0	0	0	0	0	0	0	0	0
$\xi_{12}$	0	0	0	0	0	0	0	0	0	0	0	0	0	0	0	0	0	0	1	0	0	0	0	0	0
$\xi_{31}$	0	0	0	0	0	0	0	0	0	0	0	0	0	0	0	0	0	1	0	0	0	0	0	0	0
$\xi_{23}$	0	0	0	0	0	0	0	0	0	0	0	0	0	0	0	0	1	0	0	0	0	0	0	0	0
$\xi_{14}$	0	0	0	0	0	0	0	0	0	0	0	0	0	0	0	0	0	0	0	0	$\bar{1}$	0	0	0	0
$\xi_{24}$	0	0	0	0	0	0	0	0	0	0	0	0	0	0	0	0	0	0	0	0	0	$\bar{1}$	0	0	0
$\xi_{34}$	0	0	0	0	0	0	0	0	0	0	0	0	0	0	0	0	0	0	0	0	0	0	$\bar{1}$	0	0
$\xi_{123}$	$\bar{1}$	0	0	0	0	0	0	0	0	0	0	0	0	0	0	0	0	0	0	0	0	0	0	0	0
$\xi_{124}$	0	0	0	0	0	1	0	0	0	0	0	0	0	0	0	0	0	0	0	0	0	0	0	0	0
$\xi_{314}$	0	0	0	0	0	0	1	0	0	0	0	0	0	0	0	0	0	0	0	0	0	0	0	0	0
$\xi_{234}$	0	0	0	0	0	0	0	1	0	0	0	0	0	0	0	0	0	0	0	0	0	0	0	0	0
$\xi_{1234}$	0	0	0	0	0	0	0	0	0	0	0	0	0	0	0	0	0	0	0	$\bar{1}$	0	0	0	0	0
$x^1$	0	0	0	0	0	0	0	0	0	0	0	0	0	0	1	0	0	0	0	0	0	0	0	0	0
$x^2$	0	0	0	0	0	0	0	0	0	0	0	0	0	1	0	0	0	0	0	0	0	0	0	0	0
$x^3$	0	0	0	0	0	0	0	0	0	0	0	0	1	0	0	0	0	0	0	0	0	0	0	0	0
$x^4$	0	0	0	0	1	0	0	0	0	0	0	0	0	0	0	0	0	0	0	0	0	0	0	0	0
$x^{1'}$	0	$\bar{1}$	0	0	0	0	0	0	0	0	0	0	0	0	0	0	0	0	0	0	0	0	0	0	0
$x^{2'}$	0	0	$\bar{1}$	0	0	0	0	0	0	0	0	0	0	0	0	0	0	0	0	0	0	0	0	0	0
$x^{3'}$	0	0	0	$\bar{1}$	0	0	0	0	0	0	0	0	0	0	0	0	0	0	0	0	0	0	0	0	0
$x^{4'}$	0	0	0	0	0	0	0	0	0	0	0	0	0	0	0	1	0	0	0	0	0	0	0	0	0

- 
- [1] G.'t Hooft, in "Recent Developments in Gauge Theories", p.135 Plenum Press (1980).
- [2] C.H. Albright, Phys. Rev. D**24**, 1969 (1981).
- [3] J. Terning, Phys. Rev. Lett.**80**, 2517 (1998).
- [4] F. Sannino, Phys. Rev. D**80**,065011(2009); arXiv:0911.0931[hep-th].
- [5] Y. Iwasaki, K. Kanaya, S. Sakai and T. Yoshié, Phys. Rev. Lett.**69**,21(1992).
- [6] T. Appelquist, Prog. Theor. Phys.(Kyoto)**180**,72(2009).
- [7] T. Appelquist, G.T. Fleming and E.T. Neil, Phys. Rev. Lett.**100**,171607 (2008), Phys. Rev. Lett.**102**,149902(E)(2009).
- [8] T. Appelquist, J. Terning and L.C.R. Wijewardhana, Phys. Rev. Lett.**77**,1214 (1996).
- [9] M. Luescher, R. Sommer, P. Weisz and U. Wolff, Nucl. Phys. **B143**, 481(1994).
- [10] S.J. Brodsky and R. Shrock, Phys. Lett. **B666**,95(2008),arXiv:0806.1535[hep-th].
- [11] S.J. Brodsky and G. F. de Teramond, arXiv:0804.3562[hep-ph].
- [12] S. Furui and H. Nakajima, "Infrared features of the Landau gauge QCD", Phys. Rev. D**69**,074505(2004) and references therein, arXiv:hep-lat/0305010.
- [13] S. Furui and H. Nakajima, "What the Gribov copy tells about confinement and the theory of dynamical chiral symmetry breaking", Phys. Rev. D**70**,094504(2004), arXiv:hep-lat/0403021.
- [14] S.Furui, "Propagator of the lattice domain wall fermion and the staggered fermion" ,Few-Body Syst. **45**, 51(2009), arXiv:0801.0325[hep-lat], Erratum:DOI 10.1007/s00601-009-0053-4.
- [15] S. Furui, "Roles of the color antisymmetric ghost propagator in the infrared QCD", Few-Body Systems **43** (2009), <http://dx.doi.org/10.1007/s00601-008-0005-4>; arXiv:0805.0680 [hep-lat].
- [16] C. Bernard et al.,Phys. Rev. D**64**, 054506(2001).
- [17] C. Allton et al., Phys. Rev. D**76**,014504 (2007); arXiv:hep-lat/0701013.
- [18] A. Deur, V. Burkert, J.P. Chen and W. Korsch, Phys. Lett. **B650**, 244 (2006).
- [19] A. Deur, V. Burkert, J.P. Chen and W. Korsch, Phys. Lett. **B665**,349 (2008).
- [20] J.D. Bjorken, Phys.Rev. **148**,1467(1966)
- [21] S.D. Drell and A.C. Hearn, Phys. Rev. Lett.**16**,908(1966)
- [22] S. Gerasimov, Yad. Fiz. **2**,598 (1965)
- [23] S.J. Brodsky, G.P. Lepage and P.B. Mackenzie, Phys. Rev. D**28**, 228(1983).
- [24] S.J. Brodsky and H.J. Lu, Phys. Rev. D**51**,3652 (1995).

- [25] Ph. Boucaud et al., Phys. Rev. D **66**, 034504 (2002).
- [26] K.-I. Kondo, T. Murakami, T. Shinohara, and T. Imai, Phys. Rev. D **65**, 085034 (2002).
- [27] R.D. Amado, R. Bijker and M. Oka, Phys. Rev. Lett. **58**, 654 (1987).
- [28] W. Fulton and J. Harris, *Representation Theory*, Graduate Texts in Mathematics, Springer (2004).
- [29] I.R. Porteous, "*Clifford Algebras and the Classical Groups*", Cambridge University Press (1995)
- [30] É. Cartan, "*The theory of Spinors*", p.118 Dover Pub. (1966).
- [31] E. Corrigan and P. Goddard,
- [32] H. Nakajima and S. Furui, "Numerical study of lattice Landau gauge QCD and the Gribov copy problem", Nucl. Phys. **B**(Proc.suppl.) 141, 34(2005), arXiv:hep-lat/0408001.
- [33] T. Kugo and I. Ojima, Prog. Theor. Phys.(Kyoto)Suppl. **66**, 1 (1979).
- [34] H. Nakajima and S. Furui, "A test of the Kugo-Ojima confinement criterion by lattice Landau gauge QCD simulations", Nucl. Phys. A **680**, 151c(2001).
- [35] S. Furui and H. Nakajima, "Infrared Features of Unquenched Landau Gauge QCD", Few-Body Systems **40**, 101 (2006), arXiv:hep-lat/0503029.
- [36] D. Dudal, S.P. Sorella, N. Vandersickel and H. Verschelde, Phys. Rev. D **79**, 121701(R)(2009).
- [37] K.-I. Kondo, Phys. Lett. **B678**, 322(2009).
- [38] K.I. Kondo, arXiv:0904.4897[hep-th].
- [39] S. Furui, "The Self-Dual Gauge Fields and the Domain Wall Fermion Zero Modes", Few-Body Systems **46**, 221(2009).
- [40] S. Furui, "Self-dual gauge fields, domain wall fermion zero-modes and the Kugo-Ojima confinement criterion", PoS Lattice 2009.
- [41] S. Bilson-Thompson, F.D.R. Bonnet, D.B. Leinweber, and A.G. Williams, Nucl. Phys. **B** Proc. Suppl. **109A**, 116 (2002); arXiv:hep-lat/0112034
- [42] D. Zwanziger, Nucl. Phys. **B399**, 477 (1993).
- [43] D. Zwanziger, Nucl. Phys. **B412**, 657 (1994).
- [44] M. Schaden and D. Zwanziger, hep-th:09410019 (1994).
- [45] Ph. Boucaud et al., arXiv:hep-lat/0909.2615.
- [46] V.N. Gribov, Phys. Lett. **B194**, 119(1987).
- [47] P. van Baal and N.D. Hari Dass, Nucl. Phys. **B385**, 185 (1992).